

WŁADIMIR ANTONIUK*, JERZY JAROSZEWICZ**, LESZEK RADZISZEWSKI***,
ŁUKASZ DRAGUN**

THEORETICAL STRESS ANALYSIS-BASED IMPROVEMENT OF FRICTION CLUTCH DISC MANUFACTURING PROCESS

UDOSKONALANIE PROCESU TECHNOLOGICZNEGO WYTWARZANIA TARCZ SPRZĘGIEŁ CIERNYCH NA BAZIE ANALIZY TEORETYCZNEJ STANU ODKSZTAŁCEN I NAPREŻEŃ

Abstract

Basic requirements for modern machine elements include the improvement of durability alongside the reduction of the cost of materials. This entails the need for the manufacturing process to ensure a stable geometric form of those elements. This analysis aims at developing loading schemes for the dynamic stabilization stand designed for the straightening of the discs buckled as a result of hardening heat treatment [1, 2].

Keywords: disc manufacturing process, clutch disc, spring ring, friction linings

Streszczenie

Podstawowe wymagania do współczesnych elementów maszyn to zwiększenie trwałości i obniżenie wydatku materiałowego. Wymaga to zapewnienia stabilnej formy geometrycznej elementów w trakcie procesu wytwórczego. Poniższa analiza ma na celu opracowanie schematów obciążenia dla stanowiska do dynamicznej stabilizacji prostowania tarcz, które zostały zwichrowane w wyniku obróbki cieplnej hartowania.

Słowa kluczowe: proces wytwarzania tarczy, tarcza sprzęgła, pierścień sprężysty, okładziny cierne

DOI: 10.4467/2353737XCT.16.235.5984

-
- * D.Sc. Ph.D. Eng. Władimir Antoniuk, Laboratory of Metallurgy in Mechanical Engineering, Joint Institute of Mechanical Engineering of the NAS of Belarus, Minsk.
** D.Sc. Ph.D. Eng. Jerzy Jaroszewicz, M.Sc. Eng. Łukasz Dragun, Chair of Production Management, Faculty of Management, Białystok University of Technology.
*** D.Sc. Ph.D. Eng. Leszek Radziszewski, Chair of Mechanics, Faculty of Mechatronics and Machine Design, Kielce University of Technology.

1. Theoretical analysis of strains in clutch discs

Maximum ring stresses in the spring result from maximum hub rotation. Figure 1 shows a diagram of a deformed spring.

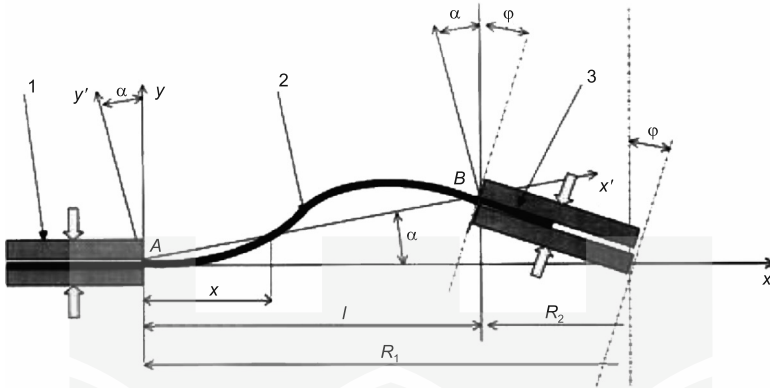


Fig. 1. Disc deformation in the maximum hub rotation plane [1]

The proposed method for stress calculation helps determine stress in any section of the disc. Here, we are interested in the value of maximum stress in the sections of maximum hub rotation and therefore a simplified stress calculation procedure can be used. Fig. 1 shows a diagram of a deformed spring in the section of the maximum angle of rotation φ . From the diagram it follows that with the hub rotation by angle φ , the spring rotates by angle α with respect to point A, and at point B, the spring rotates with respect to the hub by angle $\alpha + \varphi$. The relationships between angles α and φ are the following:

$$\operatorname{tg} \alpha = \frac{R_2}{l} \operatorname{tg} \varphi, \quad (1)$$

where:

- R_2 – is the inner radius of the spring,
- l – is the length of the spring.

Thus, maximum stress in the spring of the clutch disc occurs in the section of maximum hub angle and therefore stress calculation can be conducted only for this section. At the opposite side of the spring, stress will also occur but opposite in sign. In the section perpendicular to that under consideration, the angle of hub rotation is equal to zero and respectively all stresses are equal to zero. With one rotation of the clutch hub, the stresses on one side of the spring change direction into opposite and on the opposite side of the spring they take the value of zero twice [4].

2. Computational load scheme for the disc with a rectangular cross-section

The differential equation of the elastic surface of an annular plate in polar coordinates can have the following form [5]:

$$\left(\frac{\partial^2}{\partial r^2} + \frac{1}{r} \cdot \frac{\partial}{\partial r} + \frac{1}{r^2} \cdot \frac{\partial^2}{\partial \alpha^2} \right) \left(\frac{\partial^2 W}{\partial r^2} + \frac{1}{r} \cdot \frac{\partial W}{\partial r} + \frac{1}{r^2} \cdot \frac{\partial^2 W}{\partial \alpha^2} \right) = \frac{p}{D}, \quad (2)$$

where:

- $W = W(r, \alpha)$ – the deflection of the average plane of the plate,
- r, α – polar coordinates defining the position of the design point on the average plane,
- p – normal pressure on the plate surface,
- $D = \frac{Eh^3}{12(1-\mu^2)}$ – cylindrical rigidity of the plate,
- h – thickness of the disc,
- E – the elastic modulus of the disc material
- μ – Poisson's ratio.

Deflection W and pressure p were assumed to be positive in the downward direction. Inner moments – radial moment M_r and turning moment M_t as well as M_{rt} – the moment acting simultaneously in the radial and circumferential directions have the following forms:

$$M_r = -D \left[\frac{\partial^2 W}{\partial r^2} + \mu \left(\frac{\partial W}{r \cdot \partial r} + \frac{\partial^2 W}{r^2 \cdot \partial \alpha^2} \right) \right], \quad (3)$$

$$M_t = -D \left[\frac{\partial^2 W}{r \cdot \partial r^2} + \frac{\partial^2 W}{r^2 \cdot \partial \alpha^2} + \mu \frac{\partial^2 W}{\partial r^2} \right], \quad (4)$$

$$M_{rt} = -D(1-\mu) \left[\frac{\partial^2 W}{r \cdot \partial \alpha \cdot \partial r} - \frac{\partial W}{r^2 \cdot \partial \alpha} \right]. \quad (5)$$

To define boundary conditions we take the condition that the plate is rigidly clamped on the boundary – then deflection W and the inclination angle of the average plane of the maximum angle φ is equal to zero.

$$W = 0; \quad \frac{\partial W}{\partial r} = 0. \quad (6)$$

The general solution to homogeneous equation (5) can be expressed as a sum of general W^0 and particular W^- . The general solution of the homogeneous differential equation has the following form:

$$W^0 = F_0(r) + \sum_1^{\infty} F_m(r) \cos m\alpha + \sum_1^{\infty} f_m(r) \sin m\alpha, \quad (7)$$

Functions will be determined in accordance with the equations analogous to (8). The particular solution W^- of equation (5) is determined in each specific case according to the set law of pressure distribution on the disc surface p .

$$\left. \begin{aligned} F_0(r) &= C_{10} + C_{20}r^2 + C_{30} \ln \frac{r}{R_1} + C_{40}r^2 \ln \frac{r}{R_1} \\ F_m(r) &= C_{1m}r^m + C_{2m}r^{-m} + C_{3m}r^{m+2} + C_{4m}r^{-m+2} \quad (m \neq 1) \\ F_1(r) &= C_{11}r + C_{21}r^{-1} + C_{31}r^3 + C_{41}r \ln \frac{r}{R_1} \quad (m = 1) \end{aligned} \right\} \quad (8)$$

where:

R_1 – the outer radius of the plate.

3. Equilibrium of the disc center of symmetry

To determine the relationship between the rotation angle of the center of symmetry, φ , and the magnitude of M , the equilibrium of the disc symmetry center is considered in accordance with Figure 2.

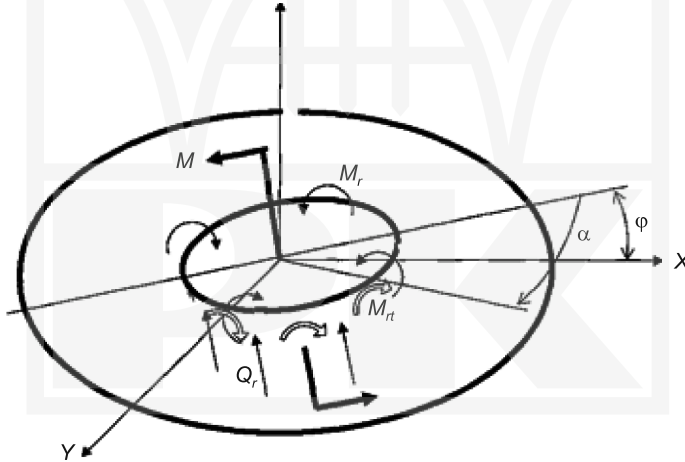


Fig. 2. Moments and forces acting on the rigid center of symmetry [1]

The rigid center is affected by the external moment M , the bending moment M_r distributed along the circumference of the radius R_2 , the torsional moment M_{rt} and the transverse force Q_r . On this basis we can write the equation of the moment with respect to axis Y [3].

$$M + \int_0^{2\pi} M_r \cdot R_2 \cdot \cos \alpha \cdot d\alpha - \int_0^{2\pi} M_{rt} \cdot R_2 \cdot \sin \alpha \cdot d\alpha + \int_0^{2\pi} Q_r \cdot R_2^2 \cdot \cos \alpha \cdot d\alpha = 0. \quad (9)$$

Quantities M_r , $M_{rr} = 0$, Q_r are defined based on (3–4). Substituting to equation (9) and taking into account that we obtain $r = R_2$ in the following way:

$$M_r = -\frac{2\varphi \cdot D \cdot (a^2 - 1) \cdot \cos \alpha}{R_2 \cdot [(a^2 + 1) \cdot \ln a - (a^2 - 1)]}, \quad Q_r = -\frac{2\varphi \cdot D \cdot (a^2 + 3) \cdot \cos \alpha}{R_2 \cdot [(a^2 + 1) \cdot \ln a - (a^2 - 1)]}. \quad (10)$$

Substituting formulas (9) in equation (10), after integration we obtain the formula for the angle of rotation necessary to attain the moment M .

$$\varphi = \frac{M[(a^2 + 1) \cdot \ln a - (a^2 - 1)]}{4\pi \cdot D \cdot (a^2 + 1)}. \quad (11)$$

The analysis indicated that the maximum value of the bending moment is (13) and occurs for coordinates $\alpha = 0$ and $r = R_2$.

$$M_{r_{\max}} = +\frac{M(a^2 - 1)}{2\pi \cdot R_2 \cdot (a^2 + 1)}. \quad (12)$$

Respective maximum stresses occur at the same point of the plate and are equal to:

$$\sigma_{\max} = +\frac{6M(a^2 - 1)}{2\pi \cdot R_2 \cdot h^2 \cdot (a^2 + 1)}. \quad (13)$$

To simplify the calculation, expressions (11), (12), (13) are written:

$$\varphi = \beta_1 \frac{M}{Eh^3}, \quad \sigma_{\max} = \beta_2 \frac{M}{R_2 \cdot h^2}, \quad M = \frac{R_2 \cdot h^2}{\sigma_{\max} \cdot \beta_2},$$

$$\beta_1 = \frac{3[(a^2 + 1) \cdot \ln a - (a^2 - 1)] \cdot (1 - \mu^2)}{\pi \cdot (a^2 + 1)}, \quad \beta_2 = \frac{3 \cdot (a^2 - 1)}{\pi \cdot (a^2 + 1)}.$$

In real service conditions, the coupling between the hub and the friction lining can have certain sensitivity and therefore expressions (11) and (13) must be supplemented with corrective factors, taking into account the sensitivity at those points. Hence, expressions (11) and (13) take the following forms [5]:

$$\varphi = \beta_1 \frac{k_3 \cdot M}{Eh^3}, \quad \sigma_{\max} = \beta_2 \frac{k_3 \cdot M}{R_2 \cdot h^2}, \quad (14)$$

where:

$k_3 = k_{\text{out}} + k_{\text{in}}$, k_{out} – the factor of decreased restraint of the disc on the outside boundary,

k_{in} – the analogous factor on the inside boundary.

We define the value of radius $r = r^*$ at which the stress in the disc is 0. This radius value corresponds to the inflection point of $W(r, \varphi)$, which can be attained using condition (15).

$$\frac{\partial^2 W(r, \varphi)}{\partial r^2} = 0. \quad (15)$$

Substituting (9) into condition (15) we obtain

$$\frac{\varphi}{a[(a^2 + 1) \cdot \ln a - (a^2 - 1)]} \left[\frac{2R_2^2 \cdot a^2}{r^3} - \frac{6r}{R_2^2} + 2(a^2 + 1) \frac{1}{r} \right] \cdot \cos \alpha = 0. \quad (16)$$

Hence, at a random angle α , condition (17) below should be satisfied:

$$\frac{R_2^2 \cdot a^3}{r^3} + \frac{a^2 + 1}{r} - \frac{3r}{R_2^2} = 0, \quad (17)$$

which can be converted into the form of the following biquadratic equation:

$$x^4 - \frac{1}{3}(a^2 + 1) \cdot x^2 - \frac{1}{3}a^2 = 0, \quad (18)$$

By solving equation (18), we find the root x corresponding to condition (15):

$$x = \sqrt{\frac{1}{6} \left[1 + a^2 + \sqrt{(a^2 + 1)^2 + 12a^2} \right]}, \quad (19)$$

where the searched radius value of zero stress in the disc is equal to:

$$r^* = R_2 \cdot \sqrt{\left\{ \frac{1}{6} \left[1 + a^2 + \sqrt{[(a^2 + 1)^2 + 12a^2]} \right] \right\}}. \quad (20)$$

4. Evaluation of the dynamic stabilization results

Table 1 summarizes the basic parameters of clutch discs on which dynamic stabilization was performed and for which the following results were obtained.

Table 1

Test results

Geometric parameters [mm]				Spring ring material	Accuracy of work surface [mm]			
D	D1	D2	b		Before modification		After modification	
					Flatness deviations	Runout	Flatness deviations	Runout
350	126	210	2	steel 45	up to 1.7	up to 2.5	0.4...0.5	0.6...0.8
340	136	210	2	steel 50	up to 1.7	up to 2.5	0.4...0.5	0.6...0.8
445	215	240	2.4	steel 45	up to 2.0	up to 3.2	0.4...0.6	0.6...0.9
316	137	156	2	steel 65H	up to 1.7	up to 2.5	0.4...0.5	0.6...0.8

5. Summary

In order to improve the geometry of clutch discs in which after heat treatment and assembly with the hub and friction linings, the spring ring exhibited considerable flatness deviations and runout of the friction surfaces, measured on the working surface, normalization of the final assembly operation is proposed – dynamic stabilization. The results of the tests indicate that the runout is reduced from 3 mm to 1 mm, which results in the decrease in the friction moment from 10 Nm to 3.5 Nm, and which occurs despite complete disengagement of the disc linings from the flywheel. Operation tests at the Tractor Factory in Minsk (Belarus) confirm that the clutch discs subjected to dynamic stabilization yield 30% higher durability and consequently, smaller number of failures.

References

- [1] Antonjuk V.E., *Dynamic stabilization of geometrical parameters of details with alternating*, Minsk: «Technoptint», 2004, 184 s.
- [2] Sandomirski S., *Primeneniye polyushnogo namagnichivaniya v magnitnom strukturnom analize (obzor)*, Defektoskopiya, vol. 9, 2006, 36-64.
- [3] Timoshenko G., Woinowsky-Krieger S., *Teoria plyt i powlok*, Arkady, Warszawa 1963.
- [4] Antonjuk V.E., Sandomirski S., Jaroszewicz J., *Issledovaniye vozmozhnostey otsenki ostotochnykh napryazheniy po gradiyentu polya ostotochnoy namagnichennosti*, Energia w Nauce i Technice, Oficyna Wydawnicza Politechniki Białostockiej, Białystok 2014.
- [5] Hoerbiger Lamellenhandbuch – A5K113/HOERBIGER Antriebstechnik GmbH // www.hoerbiger.com/Publikationen.255.0.html?&L=6 [date of access: 07.10.2010].

